

Reducing Magnetic Anisotropy Variation of Permalloy Thin Films in the dc-Magnetron Sputtering

Seungha Yoon*

Green Energy & Nano Technology R&D Group, Korea Institute of Industrial Technology, Gwangju 61012, Republic of Korea

(Received 24 April 2023, Received in final form 18 July 2023, Accepted 19 July 2023)

Considerable attention has been given to controlling magnetic anisotropy for future flexible spintronic devices because the magnetization behavior of magnetic thin film and device changes with the bending stress, which is known as the inverse-magnetostriction effect. The net magnetic anisotropy resulting from the fabrication process plays a significant role in determining the working functions for magnetic field applications. In this study, the variation of intrinsic magnetic anisotropy in permalloy thin films was investigated depending on the dc-magnetron sputtering position. The randomly formed magnetic easy-axis was finally controlled by the application of magnetic field during the sample deposition.

Keywords : magnetic anisotropy, permalloy, thin film, dc magnetron sputtering

1. Introduction

There is a significant amount of interest in the development of new materials and fabrication techniques that enable flexible electronic substrates and devices [1-4]. These flexible electronics can be found in various applications such as circuits [5], solar panels [6, 7], displays [8, 9], cell phones [10], tablets, wearable devices [11, 12], and sensors [11, 13]. Recently, there has been an increased interest in bio-applications using polymers to avoid any negative effects on human bodies, or for robots requiring attachment to curved surfaces under dynamic bending stress [14]. The flexibility of magnetism has also received a lot of attention [15-19] for the development of impact devices for imaging [20], calculators [21], and sensors [21, 22]. The magnetization of magnetic material varies when it receives bending stress, known as the inverse-magnetostriction effect or magnetomechanical effect. This effect is defined by the magnetostriction coefficient of the material and the direction of the bending stress, making it commonly used in sensor applications [23, 24]. For flexible applications, the reliable performance of bending, folding, twisting, stretching, and deforming motions is crucial. The net magnetic anisotropy

from the crystallinity [25], stress [26, 27], and pattern shape [28, 29] determines the magnetic switching behavior depending on the external magnetic field. Therefore, confirming magnetic anisotropy is important for designing flexible magnetic devices.

The aim of this study was to examine how the magnetic field applied during sputtering influences the magnetic anisotropy variation of thin magnetic films. In the absence of a magnetic field, the magnetic easy-axis of the films were randomly distributed across the sample positions. To ensure a uniform magnetic field of 460 Oe was applied to the thin films, we affixed permanent magnets onto the deposition holders. This resulted in identical magnetic hysteresis curves and improved bending properties.

2. Experimental

To demonstrate the configuration of magnetic anisotropy during the deposition, the twelve polyethylene naphthalate (PEN) substrates, each measuring 12 mm × 12 mm, were placed in a random orientation on the deposition holder, as illustrated in Fig. 1(a). The permalloy (NiFe) of 50 nm was deposited within the top and bottom 5 nm Tantalum (Ta) layers in the 5 mT working pressure. The thickness of the permalloy and Ta layers were controlled by low deposition rates of 0.11 nm/sec and 0.12 nm/sec, respectively.

A vibrating sample magnetometer (VSM) observes the

©The Korean Magnetism Society. All rights reserved.

*Corresponding author: Tel: +82-62-600-65

Fax: +82-62-600-6109, e-mail: yoonsh@kitech.re.kr

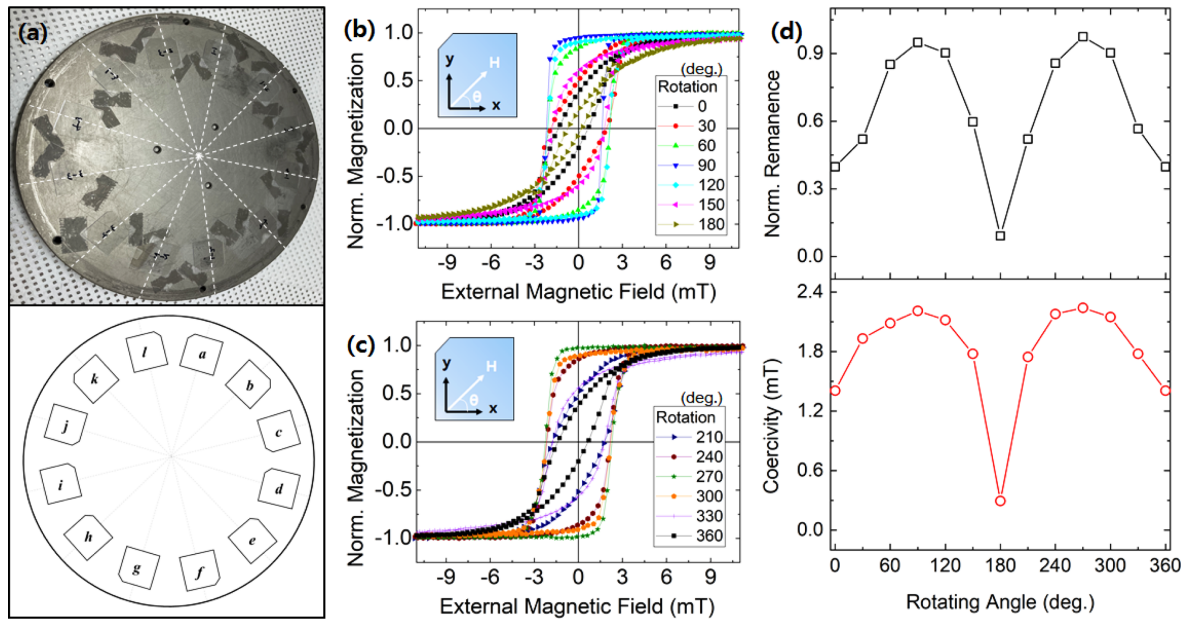


Fig. 1. (Color online) (a) The 12 randomly oriented polypropylene substrates placed on the sample holder to examine the magnetic anisotropy during the deposition process. The magnetic hysteresis loops of the "a" were measured by inducing a magnetic field from 0 to 180 degrees and 210 to 360 degrees, as displayed in (b) and (c), respectively. (d) The summary of the remanence (upper panel) and coercive field (lower panel).

magnetic moment depending on the external magnetic field in specific directions. The axis coordinators are representing the measurement geometry as shown in the inset of Fig. 1(b). The ferromagnetic resonance (FMR) method demonstrates the resonance field shift depending on the net magnetic anisotropy. To get better signal, FMR measurement performed as polypropylene substrate face-down on the co-planar waveguide channel. The Kittel equation, as shown below, indicates the in-plane FMR frequency with the intrinsic, shape, and stress-magnetic anisotropy fields [30].

$$\omega = \gamma \sqrt{(H_k + H_\sigma + H_s + H_{ext})(H_{ext} + 4\pi M_s)}$$

, where γ is the electron's gyromagnetic ratio, H_k is the intrinsic magnetic anisotropy field from the deposition process, H_σ is the magnetic anisotropy field induced by the bending stress, and H_s is the shape magnetic anisotropy field. The bending machine, which was self-designed, applied a uniform tensile stress on the film while bending it to a distance of 3 mm. Once the bending was complete and the film was released, an opposite compressive stress was applied to the film [31, 32].

3. Results and Discussion

According to the Stoner-Wohlfarth model, the remanent magnetic moment and the coercive field are strongly correlated with the magnetic anisotropy direction of the

magnetic thin film. A square-shaped hysteresis with a large coercivity is observed if the easy-axis is parallel to the external magnetic field. On the other hand, if the easy-axis is perpendicular to the external field, the magnetization gradually varies with the external field. Therefore, the magnetic easy-axis was simply determined at the angle that produced the largest magnetic remanent moment and coercivity in the hysteresis loop.

First, we measured the magnetic moment of the permalloy "a" as a function of the external magnetic field by rotating the sample from 0 to 360 degrees with respect to the field direction, as illustrated in Figs. 1(b) and (c). We observed the largest coercive field and the remanence from positive to negative saturation at 90 degrees (y-axis in the inset geometry), while the smallest coercivity and remanence were seen at 0 degrees. As per the Stoner-Wohlfarth model, the uniaxial magnetic easy-axis of the "a" permalloy thin film was demonstrated to be the y-axis. The summary of the angle dependence of coercivity and remanence is presented in Fig. 1(d).

Using the same measurement method, it was observed that the "c" permalloy thin film also had an easy-axis towards the y-axis, as shown in the upper panel of Fig. 2(a). However, the "k" thin film exhibited a tilted magnetic easy-axis at a 45 degree angle from the x-direction. In this case, the magnetic hysteresis loops were identical whether the magnetic field was applied in the x- or y-axis, as shown in the lower panel of Fig. 2(a). The magnetic

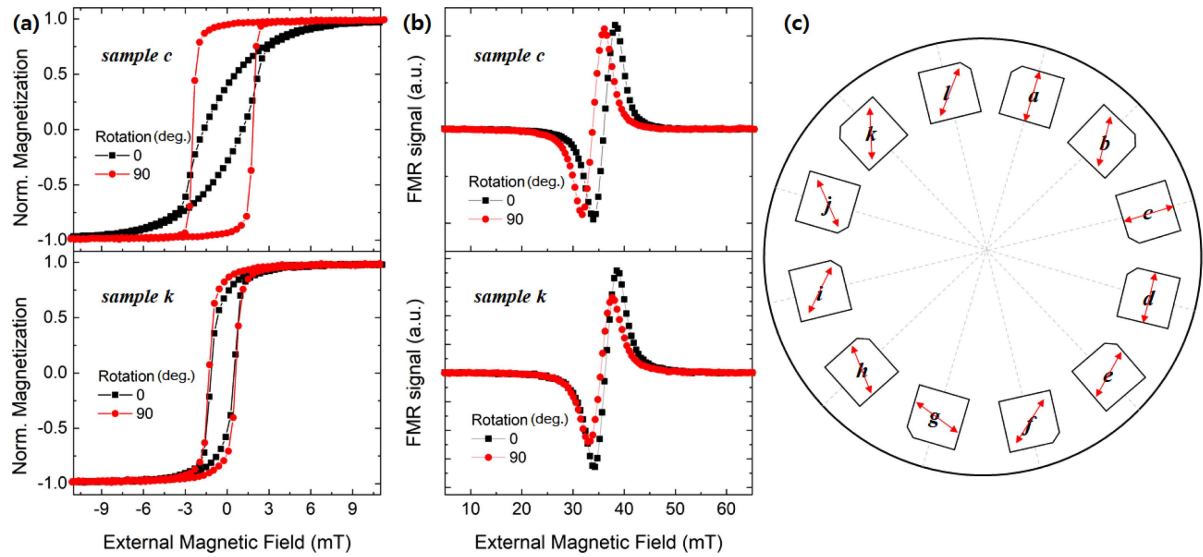


Fig. 2. (Color online) (a) The observed normalized magnetization and (b) the ferromagnetic resonance curves of "c" and "k" with the magnetic field applied at 0 and 90 degrees. (c) The easy-axis orientation of the thin films depending on the position of the sample holder.

anisotropy resulting from the dc-magnetron sputtering not only affects the magnetic hysteresis loop but also the ferromagnetic resonance absorption frequency. When a radio frequency of 5 GHz was applied to the "k" permalloy thin film, the ferromagnetic resonance field in the x-direction was found to be higher than that in the y-direction, as shown in the upper panel of Fig. 2(b). This can be attributed to the magnetic anisotropy field in the easy-axis of y-direction, which helps to reduce the external magnetic field required to generate ferromagnetic resonance. Similarly, the tilted magnetic anisotropy field resulting from the deposition produced a similar excitation magnetic field in either the x- or y-direction, as shown in the lower panel of Fig. 2(b). The magnetic easy-axis of all sample positions are shown in Fig. 2(c) with the red arrows, indicating the easy-axis through the sputtering process was randomly formed.

To achieve control over the magnetic anisotropy during the deposition process, permanent magnets were employed on the deposition holder, as shown in Fig. 3(a). The arrangement involved aligning the magnetic fields on each sample position in an outward direction from the center of the holder. Through 3D simulations, it was determined that this configuration resulted in a uniform magnetic field passing through the deposition area, as depicted in Fig. 3(b). The remanent flux density, which is a parameter of conventional NdFeB magnet, was utilized as 1.17 Tesla. Six permalloy thin films with the same thickness profile were deposited simultaneously while applying a magnetic field in the y-axis of the sample. The magnetic hysteresis loops of the films were measured

using VSM. All permalloy thin films showed easy-axis hysteresis curves when the magnetic field was applied in the y-axis (parallel to the deposition field, Fig. 3(c)), while hard-axis hysteresis loops were observed when the magnetic field was applied in the x-axis (transverse to the deposition field, Fig. 3(d)). Therefore, a well-controlled magnetic anisotropy during the deposition was achieved

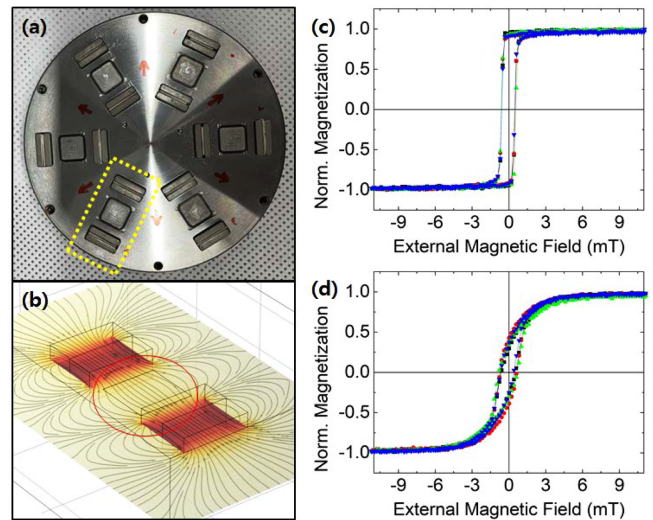


Fig. 3. (Color online) (a) The new substrate holder designed to control the magnetic anisotropy during sputtering. The holder is shown with the magnetic field applied towards the outside of the sample holder. (b) The 3D simulation demonstrates uniform magnetic field passing through the deposition area. The normalized magnetization curves of six permalloy thin films are shown in (c) and (d) for magnetic fields induced at 0 and 90 degrees, respectively.

through the design of the deposition holder using permanent magnets.

4. Conclusion

Controlling magnetic anisotropy is a crucial factor in the development of spintronic devices under magnetic fields. Intrinsic magnetic anisotropy resulting from deposition is particularly important for the fundamental functionality of these devices, and it plays a key role in reducing costs associated with additional magnetic anisotropy manipulation processes, such as field cool annealing. In this study, we investigated the intrinsic magnetic anisotropy of permalloy films during sputtering by examining their magnetic switching behaviors. The films demonstrated either easy- or hard-axis orientation to the magnetic field, with uniaxial magnetic anisotropy randomly distributed depending on the sample position on the holder. To address this, we developed a new substrate holder that utilized a magnetic field to align the magnetic moment in a specific direction. The results showed that a uniform magnetic anisotropy was achieved, and the variation in switching parameters, such as coercive field and remanence, between samples was reduced. This method has important implications for the development of spintronic devices, as controlling intrinsic magnetic anisotropy is crucial for their functionality and cost-effectiveness.

Acknowledgment

This study has been conducted with the support of the Korea Institute of Industrial Technology as "Development of core technologies of AI based self-power generation and charging for next-generation mobility (KITECH EH-23-0013)".

References

- [1] D.-Y. Khang, H. Jiang, Y. Huang, and J. A. Rogers, *Science* **311**, 208 (2006).
- [2] Y. Sun, W. M. Choi, H. Jiang, Y. Y. Huang, and J. A. Rogers, *Nat. Nanotechnol.* **1**, 201 (2006).
- [3] D. Corzo, G. Tostado-Blázquez, and D. Baran, *Front. Electron.* **1**, 594003 (2020).
- [4] P. Wang, M. Hu, H. Wang, Z. Chen, Y. Feng, J. Wang, W. Ling, and Y. Huang, *Adv. Sci.* **7**, 2001116 (2020).
- [5] H. Gleskova, S. Wagner, and D. S. Shen, *IEEE Electron Device Lett.* **16**, 418 (1995).
- [6] Z. Xing, S. Lin, X. Meng, T. Hu, D. Li, B. Fan, Y. Cui, F. Li, X. Hu, and Y. Chen, *Adv. Funct. Mater.* **31**, 2107726 (2021).
- [7] R. Zhu, Z. Zhang, and Y. Li, *Nanotechnol. Rev.* **8**, 452 (2019).
- [8] D. Zhang, T. Huang, and L. Duan, *Adv. Mater.* **32**, 1902391 (2020).
- [9] J. Park, S. Heo, K. Park, M. H. Song, J.-Y. Kim, G. Kyung, R. S. Ruoff, J.-U. Park, and F. Bien, *Npj Flex. Electron.* **1**, 9 (2017).
- [10] M. Choi, Y. J. Park, B. K. Sharma, S.-R. Bae, S. Y. Kim, and J.-H. Ahn, *Sci. Adv.* **4**, 8721 (2018).
- [11] Y. Peng, N. Yang, Q. Xu, Y. Dai, and Z. Wang, *Sensors* **21**, 5392 (2021).
- [12] H. Lim, H. S. Kim, R. Qazi, Y. Kwon, J. Jeong, and W. Yeo, *Adv. Mater.* **32**, 2070116 (2020).
- [13] B. Meng, W. Tang, Z. Too, X. Zhang, M. Han, W. Liu, and H. Zhang, *Energy Environ. Sci.* **6**, 3235 (2013).
- [14] M. Mathew, S. Radhakrishnan, A. Vaidyanathan, B. Chakraborty, and C. S. Rout, *Anal. Bioanal. Chem.* **413**, 727 (2021).
- [15] Y. Chen, X. Nie, C. Sun, S. Ke, W. Xu, Y. Zhao, W. Zhu, W. Zhao, and Q. Zhang, *Adv. Funct. Mater.* **32**, 2111373 (2022).
- [16] X. Chen and W. Mi, *J. Mater. Chem. C* **9**, 9400 (2021).
- [17] S. Zhao, Y. Zhao, B. Tian, J. Liu, S. Jin, Z. Jiang, Z. Zhou, and M. Liu, *ACS Appl. Mater. Interfaces* **12**, 41999 (2020).
- [18] T. Vemulkar, R. Mansell, A. Fernández-Pacheco, and R. P. Cowburn, *Adv. Funct. Mater.* **26**, 4704 (2016).
- [19] A. Bedoya-Pinto, M. Donolato, M. Gobbi, L. E. Hueso, and P. Vavassori, *Appl. Phys. Lett.* **104**, 062412 (2014).
- [20] R. Schmidt, A. Slobozhanyuk, P. Belov, and A. Webb, *Sci. Rep.* **7**, 1678 (2017).
- [21] M. Kondo, M. Melzer, D. Karnaushenko, T. Uemura, S. Yoshimoto, M. Akiyama, Y. Noda, T. Araki, O. G. Schmidt, and T. Sekitani, *Sci. Adv.* **6**, eaay6094 (2020).
- [22] S.-Y. Cai, C.-H. Chang, H.-I. Lin, Y.-F. Huang, W.-J. Lin, S.-Y. Lin, Y.-R. Liou, T.-L. Shen, Y.-H. Huang, P.-W. Tsao, C.-Y. Tzou, Y.-M. Liao, and Y.-F. Chen, *ACS Appl. Mater. Interfaces* **10**, 17393 (2018).
- [23] C. Herrero-Gómez, A. M. Aragón, M. Hernando-Rydings, P. Marín, and A. Hernando, *Appl. Phys. Lett.* **105**, 092405 (2014).
- [24] J.-H. Kwon, W.-Y. Kwak, and B. K. Cho, *Sci. Rep.* **8**, 15765 (2018).
- [25] P. Gruszecki, C. Banerjee, M. Mruczkiewicz, O. Hellwig, A. Barman, and M. Krawczyk, in *Solid State Phys.* (Elsevier, 2019), pp. 79-132.
- [26] F. D. Stacey, *Nature* **188**, 134 (1960).
- [27] C. T. Wolowiec, J. G. Ramírez, M.-H. Lee, N. Ghazikhanian, N. M. Vargas, A. C. Basaran, P. Salev, and I. K. Schuller, *Phys. Rev. Mater.* **6**, 064408 (2022).
- [28] L. Kopanja, M. Tadić, S. Kralj, and J. Žunić, *Ceram. Int.* **44**, 12340 (2018).
- [29] S. Oyarzún, A. Tamion, F. Tournus, V. Dupuis, and M. Hillenkamp, *Sci. Rep.* **5**, 14749 (2015).
- [30] S. J. Yuan, K. Xu, L. M. Yu, S. X. Cao, C. Jing, and J. C. Zhang, *J. Appl. Phys.* **101**, 113915 (2007).
- [31] S. Yoon, *J. Magn.* **27**, 331 (2022).
- [32] S. Yoon, *J. Magn.* **27**, 238 (2022).